NATIONAL ENVIRONMENTAL SCIENCE ACADEMY (NESA)

International Journal on Environmental Sciences
http://nesa-india.org | http://journal.nesa-india.org/index/IJES
https://doi.org/10.53390/IJES.2026.17101
IJES 17(1): 1-26 **(2026)** • ISSN: 0976-4534

PRE AND POST-MONSOON ASSESSMENT OF HEAVY METAL POLLUTION IN WATER OF RIVER GOMATI, MIDDLE GANGA BASIN

Babita Kumari[1] and Neeraj Awasthi[1]

[1]Department of Earth and Planetary Sciences
Veer Bahadur Singh Purvanchal University, Jaunpur, India

Research Paper

Received: **06.12.2025** Revised: **24.12.2025** Accepted: **05.01.2026**

ABSTRACT

Rivers are vital to human civilization but are increasingly threatened by pollution from industrial, agricultural, and domestic sources. The Gomati River, a major tributary of the Ganga in Uttar Pradesh, India, has experienced severe degradation due to rapid urbanization, industrial discharge, and poor wastewater management. This study evaluates heavy metal contamination and water quality variations along the Gomati River and its key tributaries during pre- and post-monsoon seasons of 2022. Water samples were analyzed for Fe, Ni, Cu, Zn, and Cd concentrations using Atomic Absorption Spectrophotometry, and multiple pollution indices: Metal Index (MI), Degree of Contamination (C_d), Heavy Metal Pollution Index (HPI), and Nemerow Pollution Index (NPI) were applied to assess contamination levels. Multivariate statistical tools, including Pearson correlation and Hierarchical Cluster Analysis (HCA), were used to identify inter-metal relationships and pollution sources. Results show that Cd, Ni, and Cu concentrations exceeded permissible limits at several sites, with contamination increasing downstream and peaking in the Sai tributary due to industrial and urban effluents. Pre-monsoon samples exhibited higher metal concentrations due to lower dilution and higher evaporation. Correlation and cluster analyses indicated a common anthropogenic origin of contaminants, while Caboi diagrams revealed near-neutral pH conditions favoring metal accumulation in sediments. Overall, the Gomati River system is classified as severely to critically polluted. Effective management strategies such as stricter regulation of effluent discharge, improved sewage treatment, sustainable agricultural practices, and continuous monitoring are essential to restore the ecological integrity and water quality of the Gomati River.

No. of Pages: 26 **References: 83**

Keywords: Gomati River, Heavy Metals, HPI, Caboi Diagram, Cluster Analysis, Monsoon.

INTRODUCTION

Throughout history, the growth of civilizations has largely occurred near rivers (Ahmad et al., 2010). However, rapid population expansion and the resulting dense settlements along riverbanks have led to the overuse of water resources and significant degradation of both water and sediment quality due to human activities. Surface water bodies have experienced substantial changes in both quantity and quality, driven by escalating anthropogenic pressures. These changes have disrupted aquatic ecosystems and fluvial processes, leading to the deterioration of aquatic habitats and a marked decline in biodiversity (Ugochukwu et al. 2019). The continuous discharges of untreated or

*Corresponding author: *babitabhu15@gmail.com*

partially treated industrial effluents and domestic sewage beside run-off from agricultural and mining areas into rivers have resulted in a steady increase in release of hazardous chemicals, particularly heavy metals, significantly deteriorating river water quality (Khadse et al., 2008; Sekabira et al., 2010; Lin et al. 2013).

Elements with a specific gravity greater than 5 g/cm^3 are categorized as 'Heavy metals'. Eco-toxicologists have identified approximately 20 elements e.g. mercury (Hg), lead (Pb), cadmium (Cd), chromium (Cr), zinc (Zn), arsenic (As), and nickel (Ni) along with others such as iron (Fe), copper (Cu), manganese (Mn), cobalt (Co), tin (Sn), thallium (Tl), silver (Ag), platinum (Pt), titanium (Ti), magnesium (Mg), molybdenum (Mo), selenium (Se), and bismuth (Bi) as environmental hazards due to their persistence and potential to cause harm across ecosystems (Nies, 1999; Kumar et al., 2019). Heavy metal ions exert both direct and indirect harmful effects on human health and aquatic ecosystems (Rai et al., 2015). In humans, exposure to these toxic metals can lead to a range of adverse outcomes, including physical discomfort, severe illnesses, birth defects, developmental abnormalities in fetuses, genetic mutations, cancer and irreversible damage to vital biological systems. In aquatic organisms, heavy metal contamination can result in reduced species diversity, stunted growth, and impaired reproductive capacity (Ahamad et al., 2024).

Heavy metal contamination in aquatic environments is a global concern due to the inherent toxicity of these elements, their widespread presence, persistence, and non-biodegradable nature. Their tendency to bioaccumulation in organisms and magnify through the food chain further exacerbates their ecological and health impacts (Yuan et al., 2011; Liao et al., 2017; Pushpraj and Babita., 2023). Thus, species at higher trophic levels like humans are more susceptible to harmful effects. Rivers serve as sensitive indicators of changes or disturbances in the natural state of a landscape (Schumm et al., 2000). Studies have shown that heavy metal pollution in rivers is closely linked to population growth, rapid urbanization, intensive domestic activities, expanding industrial and agricultural production as well as inadequate sanitation and wastewater treatment infrastructure (Akoto et al., 2008; Islam et al., 2014). As a result, the scarcity of clean drinkable water and declining water quality have become pressing challenges for both human sustenance and the health of aquatic ecosystems (Babiker et al., 2007). In countries like India, the uncontrolled and untreated discharge of residential/municipal and industrial wastewater and related pollutants into river catchments and urban water bodies from point sources and diffuse (non-point) sources (runoff from agricultural regions, urban areas, and homes, atmospheric deposition, construction sites, road traffic, small and large boats) further exacerbates the issue of maintaining water quality (Khadse et al., 2008; Ahmad and Khurshid, 2019; Gupta, 2020).

Heavy metals enter river systems in both dissolved (either as inorganic complexes or hydrated ions) and particulate forms. Within fluvial environments, these metals are primarily distributed among three key reservoirs: water, sediment, and biota (Maiti and Chowdhury, 2013). The concentrations of metals in each of these compartments are governed by a complex dynamic equilibrium influenced by various biological, physical and chemical processes (e.g. dissolution, precipitation, sorption, and complexion) (Saha et al., 2001). Heavy metals undergo speciation changes during their transportation. The constant interaction of heavy metals with different geochemical phases significantly affects their behavior and bioavailability and plays a critical role in determining their mobility and persistence in aquatic systems (Morillo et al., 2004; Nicolau et al., 2006). Metals are typically associated with silicates and occurring minerals, thus mineralogical composition of sediments significantly influences the natural distribution and mobility of these metals within river systems; however, anthropogenic activities can

alter their chemical associations, leading to their binding with other forms such as carbonates, oxides, and sulphides (Paramasivam et al., 2015).

Given the critical role of clean water in sustaining all forms of life, it is essential to understand the sources and behavior of heavy metals within aquatic ecosystems. In regions where river water is extensively used for drinking, agriculture, and commercial activities and where rivers are subject to significant anthropogenic pressures, regular monitoring of metal concentrations in both water and sediments is vital. Equally important is the implementation of effective management systems to assess and ensure the suitability of river water for various uses (Xiao et al., 2011; Amadi, 2011; Djordjević et al., 2012). Abeysingha et al. (2020) further emphasize the importance of formulating long-term adaptation strategies that prioritize environmental flows and ecosystem services to safeguard the sustainability of riverine systems.

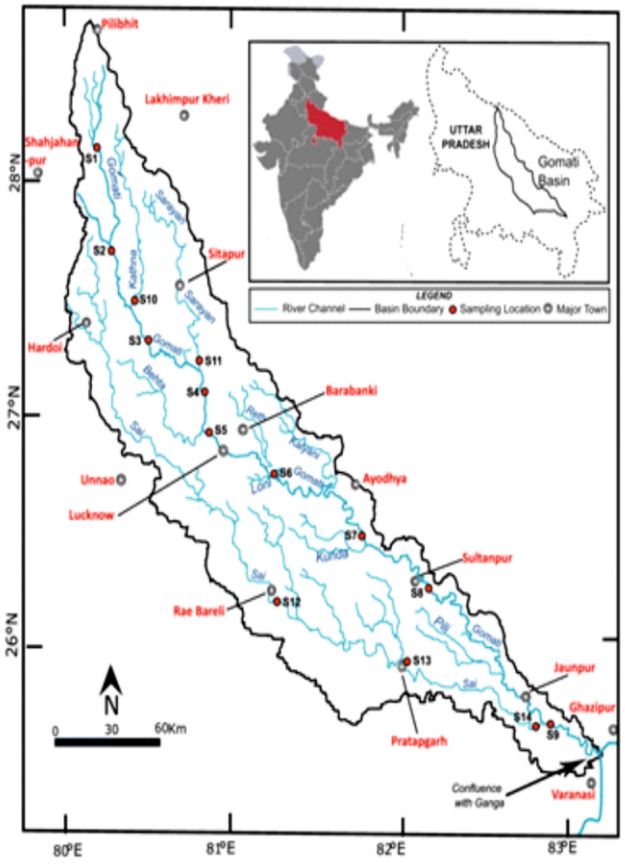

Fig. 1: Map of the Gomati River basin along with tributaries, major cities and sampling sites (modified from Kumari and Awasthi, 2025).

The Gomati River, an alluvial river in the Ganga Plain, serves as a crucial water source for numerous urban and rural settlements along its course in central and eastern Uttar Pradesh, India (Gupta et al., 2014; Gupta and Subramanian, 1994) (Fig. 1). Once in a pristine state, the river has undergone severe degradation and is now recognized as one of the most polluted rivers in the country (Singh et al., 2005). Rapid population growth, urbanization and the expansion of agricultural, industrial activities have significantly altered the natural condition of its basin, increasing pressure on its ecological balance. Previous studies have reported elevated pollution levels in the Gomati River, identifying domestic and industrial wastewater as potential sources of heavy metal contamination (Singh et al., 2005, Gaur et al. 2005; Lohani et al. 2008). However, the majority of these investigations have been limited to the Lucknow region, leaving a gap in comprehensive, basin-wide assessments. To date, no detailed seasonal analysis has been conducted to evaluate the extent of heavy metal pollution across the entire Gomati River Basin. Various pollution indices offer valuable insight into the contributions from different contamination sources. The primary objective of this study is to assess the water quality of the Gomati River along its entire course using pollution indices and other environmetric tools. The study employs multivariate statistical techniques including Pearson Correlation Analysis (PCA) and Hierarchical Cluster Analysis (HCA) to identify potential sources of heavy metal contamination, examine correlations among different metals, and evaluate spatial variability across sampling sites.

2. Samples and Methodology

2.1 Study area

The River Gomati flows through the central part of the Gangetic basin (in Uttar Pradesh, India), traversing the Ganga Plain, which is predominantly composed of sandy-silty sediments deposited during the Quaternary Period, spanning the Pleistocene to Holocene epochs (Goel, 2018). It is an alluvial tributary of the River Ganga, originating from Fulhar Jheel, a

lake located in Madhotanda village near Pilibhit, and merges with the Ganga near Varanasi, India covering a distance of approximately 940 km (Fig. 1). Unlike glacial-fed rivers, the Gomati is fed primarily by groundwater and rainfall, and originates in a marshy, forested region of the Tarai, about 50 km south of the Himalayan foothills (Kumar and Singh, 1978). Along its meandering course, the river gathers water and sediment loads from major urban centers including Lucknow (the state capital), Sultanpur, and Jaunpur, in addition to numerous smaller towns and villages spread across eight other districts: Pilibhit, Shahjahanpur, Lakhimpur, Sitapur, Barabanki, Ayodhya, Varanasi, and Ghazipur, through various small tributaries and drainage channels (Fig. 1). Among these, the River Sai is the major tributary, flowing roughly parallel and collecting runoff from Hardoi, Unnao, Raebareli, and Pratapgarh districts, before merging with Gomati at Jaunpur, just a few kilometers upstream from the Gomati's confluence with the Ganga. Other minor tributaries include Kathna, Sarayan, Behta, Reth, Luni, Kalyani, Kunda, and Pili. The River Sarayan joins Gomati near Sitapur, about 45 km upstream of Lucknow, while the Reth and Kalyani Rivers join it downstream of the city.

The River Gomati primarily redistributes Pleistocene-Holocene sediments comprising mainly sand, sandy clay, and varying amounts of calcareous nodules that were originally eroded from the Himalayas and deposited across the Ganga alluvial plain during the geological time (Singh et al., 2005). The Gomati Basin features a bas-relief landscape and gentle gradient, shaped by the combined effects of climatic fluctuations and base-level changes associated with tectonic activity (Srivastava et al., 2003). Spanning an approximate area of 30,437 km^2, the basin experiences relatively uniform climatological conditions, characterized by a semi-arid to sub-humid tropical climate with average annual rainfall ranging from 850 to 1100 mm (Dutta et al. 2011; 2015; Rai et al., 2010). The region receives nearly 75% of its total precipitation from the Indian Summer Monsoon (ISM), concentrated between June and September (Quamar et al., 2017). Seasonal temperature extremes are also notable, with summer highs reaching up to 46°C and winter lows dropping to around 2°C.

2.2 Sample collection and analysis

For this study, water samples were collected from pre-identified sites along the Gomati River and its major tributaries during two distinct seasons in 2022: pre-monsoon (May) and post-monsoon (October). Sampling was carried out at regular intervals from the river's origin to its downstream stretches, just before its confluence with the Ganga (Fig. 1). Site selection considered known discharge points for industrial effluents, domestic sewage, and solid waste, as well as the influences of major urban centers, based on insights from previous research and reconnaissance surveys (Fig. 1). The rationale for selecting these two seasons was to evaluate seasonal variation in water quality parameters and to understand how the river system either retains or flushes pollutants under contrasting hydrological conditions low flow during the summer (non-monsoon) and increased flow during the monsoon.

Water samples were collected in wide-mouth, pre-acid-washed, clean plastic bottles from nine locations along the main channel of the River Gomati: S1 (Gomat Tal/Fulhar Jheel, Pilibhit), S2 (Chapartala, Kheri), S3 (Neemsar, Sitapur), S4 (Bhatpur, Sitapur), S5 (Sitapur-Hardoi Bypass, Lucknow), S6 (Gangaganj, Lucknow), S7 (Aamghat, Amethi), S8 (Tatiyanagar, Sultanpur) and S9 (Kerakat, Jaunpur). In addition, samples were taken from five sites across major tributaries: S10 for River Kathna (Maholi, Sitapur), S11 for River Sarayan (Sidhauli, Sitapur), S12–S14 for River Sai at Raebareli, Pratapgarh, and Jaunpur, respectively, prior to its confluence with the Gomati. Sampling sites S5 and S6 represent upstream and downstream points of Lucknow city, respectively. Figure 1 illustrates the sampling locations, while Table 1 provides a brief description of each site. A handheld GPS device was used to accurately record the coordinates of each sampling location as given in Kumari and Awasthi, (2025). The study covered an approximate 900 km stretch of

Table 1: Sampling locations of the river water samples collected from the Gomati main channel and its tributaries with expected sources of heavy metal pollution.

Sample No.	Sampling Locations	Distance from the origin (km)	Expected sources of pollution
Gomati Main Channel			
S1.	Gomat Tal/Fulhar Jheel (Pilibhit)	0	Agricultural
S2.	Chapartala (Kheri)	206	Agricultural
S3.	Neemsar (Sitapur)	304	Agricultural
S4.	Bhatpur (Sitapur)	373	Agricultural, Industrial effluents & Domestic wastewater
S5.	Sitapur-Hardoi Bypass (Lucknow)	425	Agricultural, Industrial effluents & Domestic wastewater
S6.	Gangaganj (Lucknow)	496	Agricultural, Industrial effluents & Domestic wastewater
S7.	Aamghat, Jagdishpur (Amethi)	650	Agricultural, Industrial effluents & Domestic wastewater
S8.	Tatiyanagar (Sultanpur)	736	Agricultural, Industrial effluents & Domestic wastewater
S9.	Kerakat (Jaunpur)	915	Agricultural, Industrial effluents & Domestic wastewater
Tributary Kathna			
S10.	Maholi (Sitapur)	270	Agricultural, Industrial effluents & Domestic wastewater
Tributary Sarayan			
S11.	Sidhauli (Sitapur)	371	Agricultural, Industrial effluents & Domestic wastewater
Tributary Sai			
S12.	Dariyapur (Raebareli)	323 before confluence with Gomati	Agricultural, Industrial effluents & Domestic wastewater
S13.	Chilbila (Pratapgarh)	135 before confluence with Gomati	Agricultural, Industrial effluents & Domestic wastewater
S14.	Sarkoni (Jaunpur)	902	Agricultural, Industrial effluents & Domestic wastewater

the Gomati River, enabling an assessment of heavy metal (HM) pollution across upstream, midstream, and downstream zones.

A total of 28 water samples were collected during the study 14 samples, each in the pre-monsoon and post-monsoon seasons. Additionally, three duplicate samples were collected from sites S3, S6, and S9 to ensure analytical precision. Prior to collection, all pre-labeled 1-liter plastic bottles were thoroughly rinsed multiple times with the respective sample water. Sampling, transportation, preservation, and analysis followed standard protocols as recommended by the American Public Health Association (APHA, 2017), Bureau of Indian Standards (BIS, 2012), and World Health Organization (WHO, 2017) guidelines. For heavy metal analysis, water

samples were first digested with concentrated nitric acid (HNO_3). The processed samples were then tested for six metals Fe, Ni, Zn, Cu, and Cd using a Flame Atomic Absorption Spectrophotometer, along with reagent blanks and standard solutions for accuracy. These metals were chosen based on findings from earlier studies on surface water pollution and the available laboratory facilities. All chemicals used were of analytical grade and sourced from Merck, India. Double-distilled water was used in all preparations, and all glassware was rigorously cleaned using deionized water and 2% HNO_3 to prevent contamination. To ensure data reliability, quality control and assurance protocols were implemented, including blank checks, standard verifications, and duplicate analyses. The accuracy and precision of the results were validated through repeated analyses of both samples and standards.

2.3 Estimation of Pollution Indices

2.3.1 Metal index (MI) and Degree of contamination (C_d)

The metal index (MI) is estimated using the equation 1 as follows:

$$MI = \sum_{i=1}^{n} Ci / MACi \quad \ldots\ldots 1$$

Where MI represents the Metal Index, Ci is the concentration of the i-th metal in the water sample, MACi is the maximum allowable concentration for that metal and i refer to each individual metal or sample component included in the calculation. This index provides a cumulative assessment of metal contamination by comparing observed concentrations to established safety thresholds. According to Caeiro et al (2005), MI< 0.3 is categorized as very pure (Class I), 0.3 to 1.0 is categorized as pure (Class II), 1.0 to 2.0 is slightly affected (Class III), 2.0 to 4.0 moderately affected (Class IV), 4.0 to 6.0 strongly affected (Class V) and > 6.0 is seriously affected (Class VI).

The impact of heavy metals on surface water quality can be measured using the degree of contamination (C_d) (Li *et al.*, 2015, 2016), calculated with the following equations:

$$C_d = \sum_{i=1}^{n} Cfi \quad \ldots\ldots 2$$

$$Cfi = (Mi/Si) - 1 \quad \ldots\ldots 3$$

Here, Cfi is the contamination factor of the ith heavy metal, Mi is its measured concentration, and Si is the standard permissible limit. According to Edet & Offiong, (2002) based on C_d values, water quality is classified as: Low pollution: $C_d < 1$, Moderate pollution: $1 < C_d < 3$, High pollution: $C_d > 3$.

2.3.2 Heavy metal pollution index (HPI)

The Heavy Metal Pollution Index (HPI) is a valuable tool for evaluating the overall water quality with respect to heavy metal contamination (Sheykhi and Moore, 2012). It functions as a weighted arithmetic index, similar in concept to the Water Quality Index (WQI) and is calculated in two primary steps: (1) by assigning relative weights to selected heavy metal that is typically inversely proportional to their permissible limit parameters and (2) quantify their combined impact on surface water quality by developing a rating scale based on those parameters (Mohan et al., 1996). The rating scale typically ranges from 0 to 1 and the selection of parameters is based on their significance in determining water quality. These rating values can also be determined by establishing an inverse proportional relationship with the standard permissible limits for each parameter (Horton, 1965). The unit weight (Wi) assigned to each parameter is inversely proportional to its respective standard value (Si), as described by equation (4):

$$HPI = \sum_{i=1}^{n} WiQi / \sum_{i=1}^{n} Wi \quad \ldots\ldots 4$$

where n denotes the number of heavy metals used in the present study; Wi is unit weight of ith heavy metal. The subindex (Qi) is calculated from equation (5):

$$Qi = \sum_{i=1}^{n} ((Mi(-)Ii)/(Si - Ii)) \times 100 \quad \ldots\ldots 5$$

In this context, Mi (µg/L) represents the measured concentration of the ith heavy metal, Si is its standard permissible limit, and Ii is the ideal value for that metal in drinking water, as specified by BIS (2012) and Prasad & Bose (2001). Earlier studies applied a single threshold value of HPI = 100 to categorize water as "Critically Polluted" (Prasad & Bose, 2001). However, a more

refined classification system is now widely used, introduced by Edet and Offiong (2002), which categorizes HPI values into three levels of pollution: low (< 15), medium (15–30), and high (> 30). However, if HPI values go higher than 100, the sites are considered "critically polluted". In the present study, HPI has been computed to evaluate the extent of heavy metal pollution in the Gomati River, focusing on selected heavy metals across multiple sites.

2.3.3 Nemerow pollution index (NPI)

The Nemerow Pollution Index (NPI) is another widely used method for evaluating the overall pollution level at a given site, especially in the context of heavy metal contamination in water. It integrates both the maximum individual pollution index and the average pollution index across multiple pollutants to provide a more comprehensive assessment of environmental quality (Su et al., 2022). By accounting for the most severe as well as average of the single factor indices, which accurately represents the degree of water pollution, and the more polluting indicators, the NPI offers a balanced representation of site-wide pollution. This makes NPI more thorough when evaluating water quality than the single factor index method. This unitless numerical value is easy to interpret and effective in identifying polluted areas and prioritizing remediation strategies. The NPI is calculated using the following formula:

$$NPI=\sqrt{((Avg\ Pi)^2+(max\ Pi)^2)/2} \quad \ldots\ldots (6)$$

Where NPI is the overall pollution index for a sampling site, max Pi is the highest value among the individual pollution indices, Avg Pi = $1/n\sum n\ i=1Pi$ is the mean of the single-factor pollution indices, with n being the number of pollutants analyzed. Pollution severity based on NPI is typically categorized into four levels: Class I: NPI ≤ 0.7 — Clean or unpolluted, Class II: 0.7 < NPI ≤ 1 — Slight pollution, Class III: 1 < NPI ≤ 2 — Moderate pollution, Class IV: 2 < NPI > 3 — Heavy pollution, Class V: NPI > 3 — Serious pollution.

The NPI was used to analyze the level of pollution of a single water quality parameter in relation to standard values and to evaluate the effects of multiple pollutants on a specific water body. Each location index therefore reflects both the highest relative evaluated value and the average of all relative values. The NPI was used to assess pollution levels for individual water quality parameters compared to standard values and to evaluate the combined effect of multiple pollutants on the river. At each site, the index reflects both the highest pollutant value and the overall average, giving a balanced view between the worst and average conditions (Nemerow, 1991).

2.4 Pearson correlation matrix (PCA) and Hierarchical Cluster analysis (HCA)

The multivariate statistical methods such as PCA and HCA have proven to be effective tools in water quality assessment. To assess seasonal effects on water quality, Pearson's correlation coefficient (r) was calculated for heavy metals using Microsoft Excel software. This statistical method measures the strength and direction of linear relationships between variables, helping to identify interrelated water quality parameters that may influence overall water conditions. The correlation coefficient (r) ranges from +1 to -1 where +1 indicates a perfect positive linear relationship, -1 indicates a perfect negative linear relationship, and 0 suggests no linear correlation. A positive correlation implies that an increase in one metal is associated with an increase in another, while a negative correlation indicates the opposite. The strength of correlation either negative or positive was categorized as follows: very strong: 0.9–1.0, strong: 0.7–0.9, moderate: 0.5–0.7, weak: 0.5–0.3, negligible: 0.00–0.3 (Schober, et al., 2018). This analysis helps determine which metal concentrations tend to vary together, offering insights into possible common sources or environmental behaviors. Hierarchical Cluster Analysis (HCA) was carried out using PAST 4.0 software. The analysis used Ward's method with squared Euclidean distance to group samples by minimizing differences within each cluster. HCA, especially when applied using Ward's linkage method, efficiently groups water quality parameters based on internal similarities and external dissimilarities among

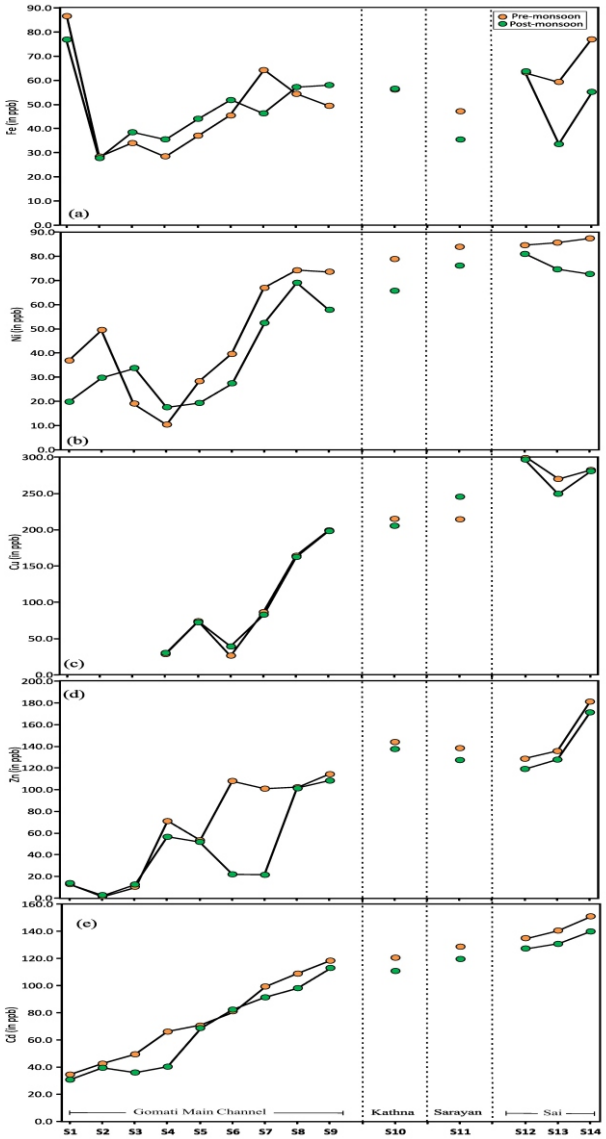

Fig. 2: Heavy metal concentrations (in μg/L) in the Gomati main channel (S1–S9) and tributaries [Kathna (S10), Sarayan (S11), Sai (S12-S14)] for (a) Fe (b) Ni (c) Cu (d) Zn (e) Cd. The pre- and post-monsoon data are represented in orange and green circles, respectively. Dashed vertical lines separate river sections and tributaries.

clusters (Gupta et al., 2014). As a result, the technique is widely used to identify patterns in water quality variation and analyze complex datasets as well as interpret the potential sources of heavy metal contamination in river systems (Mishra et al., 2015).

25 Caboi diagram

Water samples were also classified using the method by Caboi et al. (1999), which is based on pH and metal load (μg/L). The various metal load categories expressed in the Caboi diagram are "near neutral-low metal," "acid-high metal," "near neutral high metal," "near neutral-extreme metal," and "high acid-extreme metal". A lower pH corresponds to a higher metal load, increasing the mobility of heavy metals in water under acidic conditions (Singh et al., 2017).

3. Results

3.1 Distribution of heavy metals

Table 2 presents the summary of heavy metal minimum, maximum, average and standard deviation values in water samples from all sites. Of the nine metals analyzed, five (Fe, Ni, Cu, Zn, Cd) were detected, while Mn, Cr, Co, and As were either absent in our samples or below detection limit. The results of heavy metal concentrations in the river water samples analyzed are plotted in Figure 2. Except at some sites, the data for Ni, Cu, Zn and Cd shows increasing trend with downstream locations. Fe behaved differently and show fluctuations in its concentrations at different sites and during different seasons. However, in each case the concentrations of metals in tributaries were higher than the main channel. The measured values ranged as follows: pH from 7.8 to 8.4 (Average: 8.0) for pre-monsoon and 7.2 to 8.4 (Average: 7.9) for post-monsoon, Fe from 28.5 to 86.6 μg/L (Average: 50.6 μg/L) for pre-monsoon and from 27.9 to 76.9 μg/L (Average: 48.8 μg/L) for post-monsoon, Ni from 10.6 to 87.6 μg/L (Average: 56.1 μg/L) for pre-monsoon and from 13.0 to 81.1 μg/L (Average: 48.2 μg/L) for post-monsoon, Cu from 24.4 to 299.3 μg/L (Average: 160.8 μg/L) for pre-monsoon and from 28.9 to 297.3 μg/L (Average: 162.2 μg/L) for post-monsoon, Zn from 2.0 to 181.6 μg/L (Average: 90.6 μg/L) for pre-monsoon and from 3.1 to 71.9 μg/L (Average: 171.6 μg/L) for post-monsoon. Cd from 34.8 to 151.3 μg/L (Average: 94.1 μg/L) for pre-monsoon and from 26.1 to 140.2 μg/L (Average: 86.4 μg/L) for post-monsoon.

3.2 Pollution Indices

Figure 3 shows the classification and water quality distribution in the Gomati and its

Table 2: Statistical summary of analytical results of heavy metals measured in this work, compared to values acceptable by Bureau of Indian Standards (BIS) in surface waters for drinking purpose.

Parameters	Pre-Monsoon			Post-Monsoon			Standard values
	Max	Min	Average ± sd	Max	Min	Average ± sd	
pH	8.4	7.8	8.0 ± 0.2	8.4	7.2	7.9 ± 1.0	6.5–8.5$
Fe	86.6	28.5	50.6 ± 16.3	76.9	27.9	48.8 ± 12.8	300$
Ni	87.6	10.6	56.1 ± 26.9	81.1	13	48.2 ± 24.1	20$
Cu	299.3	24.4	160.8 ± 100.5	297.3	28.9	162.2 ± 97.5	1500$
Zn	181.6	2.0	90.6 ± 54.4	171.6	3.1	71.9 ± 55.7	15000$
Cd	151.3	34.8	94.1 ± 37.3	140.2	26.1	86.1 ± 37.8	3$

All concentrations are expressed in (µg/L); sd: standard deviation, $BIS (2012)

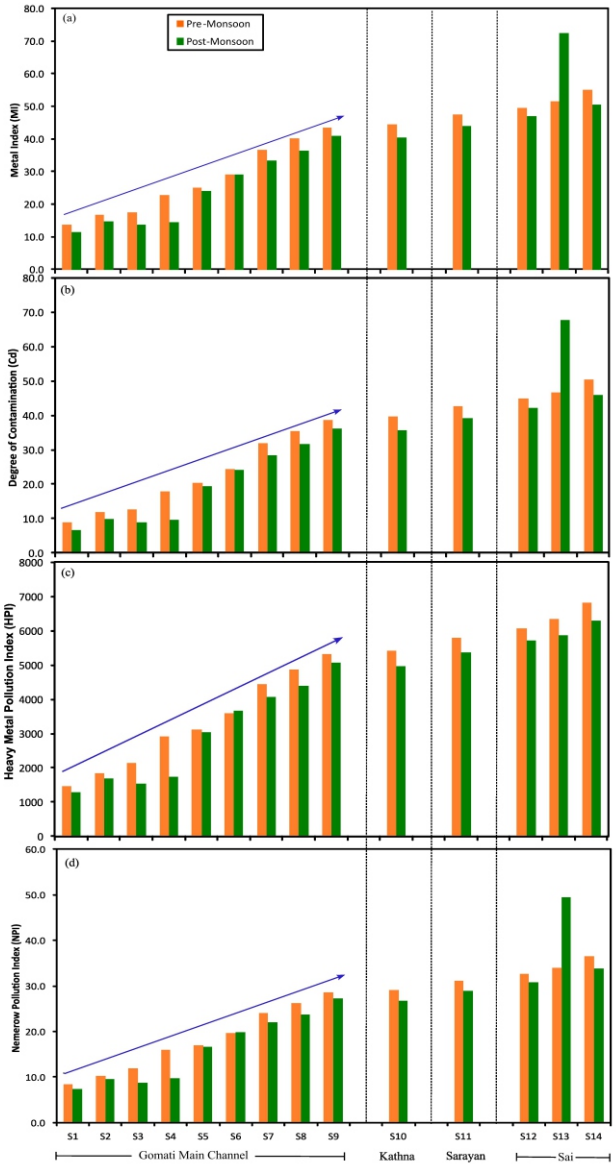

Fig. 3 Variations of different metal indices calculated using heavy metal concentrations in the Gomati main channel and tributaries (a) Metal Index (b) Degree of contamination (c) Heavy Metal Pollution Index (d) Nemerow Pollution Index.

tributaries based on MI, C_d, HPI, and NPI, the calculation and values for which are shown in Supplementary Tables S1 and S2. The MI values ranged from 13.7 to 55.3 in the pre-monsoon and from 11.6 to 72.6 in the post-monsoon (Fig. 3a). The lowest value was recorded at site S1 in both seasons, while the highest was at S14 (pre-monsoon) and S13 (post-monsoon). For C_d, values ranged from 8.7 to 50.3 in the pre-monsoon and 6.6 to 67.6 in the post-monsoon, with mean values of 30.3 and 28.9, respectively (Fig. 3b). HPI increased along the Gomati River from upstream locations to downstream, mainly due to pollution received from midstream tributaries and drains (Fig. 3c). During the pre-monsoon, HPI followed the order S1 < S2 < S3 < S4 < S5 < S6 < S7 < S8 < S9 < S10 < S11 < S12 < S13 < S14, with the lowest pollution at S1 and the highest at S14. The post-monsoon pattern was similar, except for a slight change between S2 and S3. Like HPI, the NPI method proved effective in showing the overall condition of the river (Fig. 3d).

3.3 Correlation and Cluster Analysis

Table 3 presents Pearson correlation matrices for six water quality parameters (pH, Fe, Ni, Cu, Zn, and Cd) and metal indices calculated using heavy metal concentrations during pre- and post-monsoon seasons. In the pre-monsoon period, Fe shows moderate positive correlation with Ni (r = 0.52) and strong positive correlation with Cu (r = 0.71). Ni is strongly positively correlated with Cu (r = 0.88), Zn (r = 0.77), and Cd (r = 0.87). Cu also has strong positive correlations with Zn (r =

Table 3: Heat map of Pearson's correlation matrix between various heavy metals measured in Gomati River during pre- and post-monsoon periods and estimated pollution indices.

PRE-MONSOON	pH	Fe	Ni	Cu	Zn	Cd	MI	NPI	HPI	C_d
pH	1.00									
Fe	-0.41	1.00								
Ni	-0.46	0.52	1.00							
Cu	-0.46	0.71	0.88	1.00						
Zn	-0.42	0.39	0.77	0.79	1.00					
Cd	-0.51	0.37	0.87	0.96	0.95	1.00				
MI	-0.51	0.40	0.89	0.95	0.95	1.00	1.00			
NPI	-0.51	0.37	0.87	0.96	0.95	1.00	1.00	1.00		
HPI	-0.51	0.37	0.87	0.96	0.95	1.00	1.00	1.00	1.00	
C_d	-0.51	0.40	0.89	0.95	0.95	1.00	1.00	1.00	1.00	1.00
POST-MONSOON	pH	Fe	Ni	Cu	Zn	Cd	MI	NPI	HPI	C_d
pH	1.00									
Fe	0.01	1.00								
Ni	-0.21	0.11	1.00							
Cu	-0.14	0.29	0.92	1.00						
Zn	-0.06	0.15	0.83	0.90	1.00					
Cd	-0.31	0.14	0.90	0.93	0.87	1.00				
MI	-0.43	-0.01	0.85	0.81	0.81	0.93	1.00			
NPI	-0.44	-0.02	0.83	0.79	0.80	0.92	1.00	1.00		
HPI	-0.31	0.14	0.90	0.93	0.87	1.00	0.93	0.92	1.00	
C_d	-0.43	-0.01	0.85	0.81	0.81	0.93	1.00	1.00	0.93	1.00

*The values range from -1 to +1 and are color-coded where dark green signifies very strong positive correlations, dark red signifies very strong negative correlations, intermediate shades of yellow and orange show strong, moderate to weak correlations).

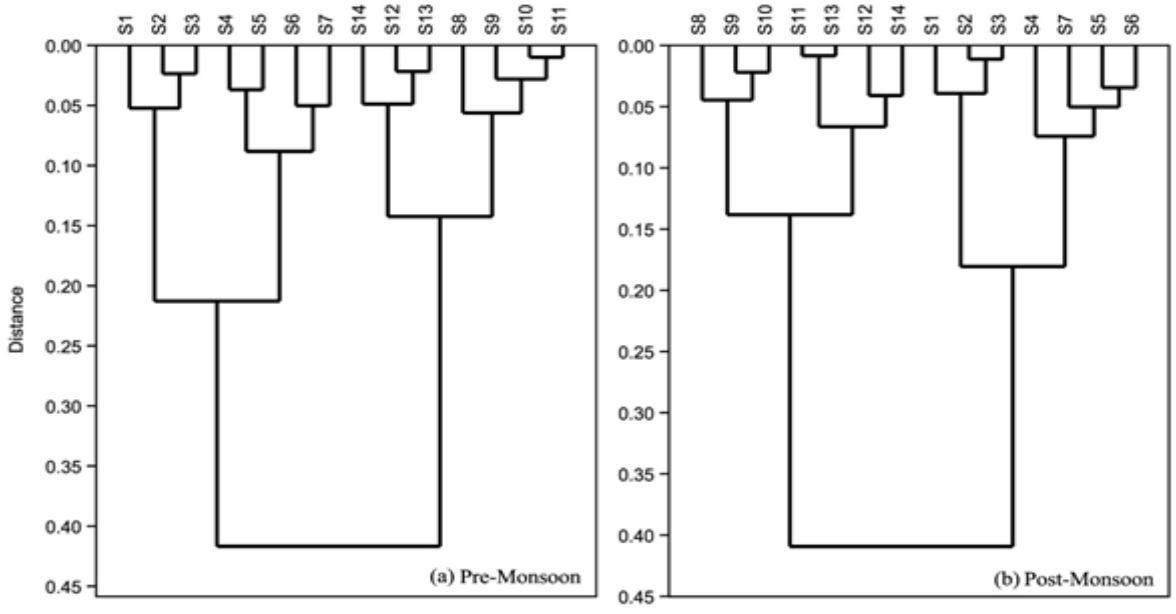

Fig. 4: The dendrogram obtained from hierarchical clustering analysis for sampling sites during (a) pre-monsoon (b) post-monsoon.

0.79) and an extremely strong one with Cd (r = 0.96); Cd and Zn are similarly vary strongly positively correlated (r = 0.95). In the post-monsoon season, very strong positive correlations are observed between Cu and Ni (r = 0.92), Cu and Cd (r = 0.93), and Ni and Cd (r = 0.90). Zn also shows strong positive correlations with Ni (r = 0.83) and Cd (r = 0.87). Metal indices like MI, C_d, HPI, and NPI also show very strong to strong positive correlations with Cd, Zn, Cu and Ni suggesting their decisive roles in estimation of these pollution indices and degradation of the water quality.

HCA was performed to understand the similarity among the parameters that contribute largely in contaminating water with heavy metals. HCA grouped the sampling sites into three major clusters in both pre- and post-monsoon seasons, though the site composition within clusters varied. HCA using Ward's method on the pre-monsoon data, group sampling sites into three clusters based on similarities in water quality within these groups (Fig. 4a): HCA1: sites S1–S7 formed one large cluster; HCA2: S12–S14 grouped together and forms another cluster; HCA3: S8–S11 clustered separately. In contrast, during the post-monsoon (Fig. 4b), sites HCA1: S8–S14 merged into a single larger cluster, while upstream sites HCA2: (S1–S4, S7) and midstream sites HCA3: S5–S6 formed two distinct groups. During both the seasons, heavy metals were grouped into two clusters: Cluster 1: Zn, Cd, Fe, Ni; Cluster 2: Cu (not shown).

3.4 Caboi diagram

Water samples were categorized using the Caboi diagram (Caboi et al., 1999; Ficklin et al., 1992) based on pH and total dissolved metal load (Fe + Ni + Cd + Zn + Cu). Since metal precipitation and release depends on pH, the near-neutral to alkaline nature suggests heavy metals likely should settle in sediments as carbonates or oxides (Singh et al., 2005). In this study, water pH for the Gomati main channel and tributaries ranged from 7.6 to 8.3 (pre-monsoon) and 6.1 to 10.6 (post-monsoon), generally indicating neutral to alkaline conditions, within WHO limits (Fig. 5). However, extreme pH values were observed post-monsoon in tributaries Kathna (high: 10.6) and Sai at Pratapgarh (low: 6.1).

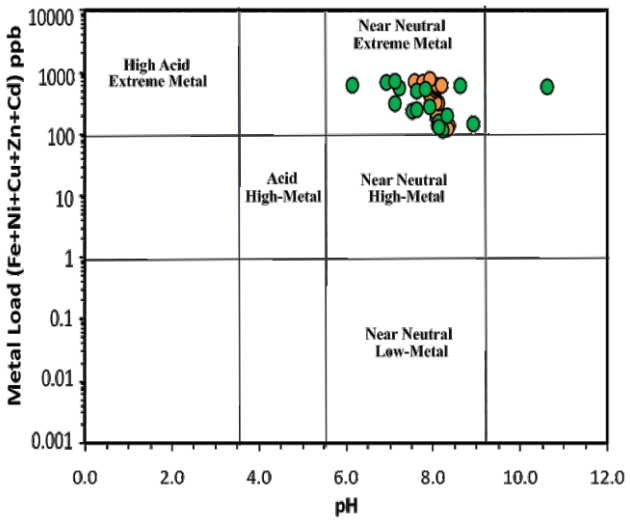

Fig. 5: Caboi diagram representing the mobility of heavy metals in the Gomati main channel and tributaries with the variation in pH. Orange circles are for pre-monsoon data and green circles for post-monsoon data.

4. Discussion

Although sampling seasons differed, some of our locations overlapped with study by Singh et al. (2005). Comparing our data with that study, we observed that except Fe, the concentrations of all heavy metals were much higher in pre- and post-monsoon seasons of 2022. Fe was previously reported as 79–319 μg/L (Singh et al., 2005), 102–339 μg/L (Khan et al., 2020), and 92–270 μg/L (Khan et al., 2021). However, in 2022, Fe levels were lower during both the seasons (28–87 μg/L, pre-monsoon and 28–77 μg/L, post-monsoon). Fe concentration is highest at the origin of the Gomati River (S1, Madho Tanda) during both seasons, but it decreases at S2 and then shows fluctuating values with a general increase downstream (Fig. 2a). Higher Fe levels are found at downstream stations (S7–S9) and again in the Sai tributary (S12–S14). Post-monsoon Fe values are slightly lower than pre-monsoon ones at most sites, indicating dilution caused by rainfall and surface runoff. The concentrations in tributaries such as Kathna (S10) and Sarayan (S11) are

Table 4: Estimation of Metal index (MI) and Degree of contamination (C_d) for different sampling sites of the Gomati River main channel and tributaries.

		Pre-Monsoon					Post-Monsoon				
Samples/ Symbols	**Maximum Allowable conc. (MAC) in ppb**	**Mean conc. (Ci) in ppb**	**Ci/MAC**	**Metal Index**	**Cfi**	**Degree of contamination C_d**	**Mean conc. (Ci)**	**Ci/MAC**	**Metal Index**	**Cfi**	**Degree of contamination C_d**
S1											
Fe	300	86.60	0.29	**13.73**	-0.711	**8.73**	76.91	0.26	**11.59**	-0.744	**6.59**
Ni	20	37.07	1.85		0.853		20.00	1.00		0.000	
Cu	1500	0.00	0.00		-1.000		0.00	0.00		-1.000	
Zn	15000	13.17	0.00		-0.999		13.73	0.00		-0.999	
Cd	3	34.75	11.58		10.584		30.99	10.33		9.329	
S2											
Fe	300	28.50	0.10	**16.83**	-0.91	**11.83**	27.90	0.09	**14.84**	-0.91	**9.84**
Ni	20	49.70	2.49		1.49		29.93	1.50		0.50	
Cu	1500	0.00	0.00		-1.00		0.00	0.00		-1.00	
Zn	15000	2.03	0.00		-1.00		3.06	0.00		-1.00	
Cd	3	42.76	14.25		13.25		39.75	13.25		12.25	
S3											
Fe	300	34.08	0.11	**17.64**	-0.89	**12.64**	38.56	0.13	**13.92**	-0.87	**8.92**
Ni	20	19.26	0.96		-0.04		33.95	1.70		0.70	
Cu	1500	0.00	0.00		-1.00		0.00	0.00		-1.00	
Zn	15000	10.77	0.00		-1.00		12.81	0.00		-1.00	
Cd	3	49.69	16.56		15.56		36.27	12.09		11.09	
S4											
Fe	300	28.60	0.10	**22.78**	-0.90	**17.78**	35.63	0.12	**14.55**	-0.88	**9.55**
Ni	20	10.58	0.53		-0.47		17.73	0.89		-0.11	
Cu	1500	29.01	0.02		-0.98		29.47	0.02		-0.98	
Zn	15000	71.33	0.00		-1.00		56.80	0.00		-1.00	
Cd	3	66.40	22.13		21.13		40.57	13.52		12.52	
S5											
Fe	300	37.17	0.12	**25.20**	-0.88	**20.20**	44.13	0.15	**24.19**	-0.85	**19.19**
Ni	20	28.51	1.43		0.43		19.50	0.98		-0.03	
Cu	1500	74.37	0.05		-0.95		74.03	0.05		-0.95	
Zn	15000	53.67	0.00		-1.00		52.14	0.00		-1.00	
Cd	3	70.79	23.60		22.60		69.03	23.01		22.01	
S6											
Fe	300	45.52	0.15	**29.30**	-0.85	**24.30**	51.88	0.17	**29.08**	-0.83	**24.08**
Ni	20	39.78	1.99		0.99		27.63	1.38		0.38	
Cu	1500	26.94	0.02		-0.98		0.00	0.00		-1.00	
Zn	15000	108.37	0.01		-0.99		22.25	0.00		-1.00	
Cd	3	81.40	27.13		26.13		82.59	27.53		26.53	
S7											
Fe	300	64.26	0.21	**36.84**	-0.79	**31.84**	46.39	0.15	**33.39**	-0.85	**28.39**
Ni	20	67.10	3.36		2.36		52.60	2.63		1.63	
Cu	1500	86.93	0.06		-0.94		83.40	0.06		-0.94	
Zn	15000	101.23	0.01		-0.99		21.77	0.00		-1.00	
Cd	3	99.63	33.21		32.21		91.63	30.54		29.54	

S8											
Fe	300	54.43	0.18	**40.39**	-0.82	**35.39**	57.27	0.19	**36.57**	-0.81	**31.57**
Ni	20	74.37	3.72		2.72		69.20	3.46		2.46	
Cu	1500	164.60	0.11		-0.89		163.00	0.11		-0.89	
Zn	15000	102.56	0.01		-0.99		102.00	0.01		-0.99	
Cd	3	109.11	36.37		35.37		98.40	32.80		31.80	
S9											
Fe	300	49.52	0.17	**43.54**	-0.83	**38.54**	58.08	0.19	**40.87**	-0.81	**35.87**
Ni	20	73.76	3.69		2.69		58.03	2.90		1.90	
Cu	1500	199.62	0.13		-0.87		0.00	0.00		-1.00	
Zn	15000	114.60	0.01		-0.99		108.68	0.01		-0.99	
Cd	3	118.65	39.55		38.55		113.30	37.77		36.77	
S10											
Fe	300	56.23	0.19	**44.57**	-0.81	**39.57**	56.41	0.19	**40.65**	-0.81	**35.65**
Ni	20	79.03	3.95		2.95		65.90	3.30		2.30	
Cu	1500	215.50	0.14		-0.86		205.90	0.14		-0.86	
Zn	15000	144.29	0.01		-0.99		137.80	0.01		-0.99	
Cd	3	120.83	40.28		39.28		111.07	37.02		36.02	
S11											
Fe	300	47.27	0.16	**47.50**	-0.84	**42.50**	35.57	0.12	**44.06**	-0.88	**39.06**
Ni	20	84.06	4.20		3.20		76.30	3.82		2.82	
Cu	1500	214.87	0.14		-0.86		246.00	0.16		-0.84	
Zn	15000	138.67	0.01		-0.99		127.63	0.01		-0.99	
Cd	3	128.96	42.99		41.99		119.87	39.96		38.96	
S12											
Fe	300	63.27	0.21	**49.73**	-0.79	**44.73**	63.50	0.21	**47.02**	-0.79	**42.02**
Ni	20	84.73	4.24		3.24		81.13	4.06		3.06	
Cu	1500	299.33	0.20		-0.80		297.33	0.20		-0.80	
Zn	15000	128.88	0.01		-0.99		119.43	0.01		-0.99	
Cd	3	135.23	45.08		44.08		127.63	42.54		41.54	
S13											
Fe	300	59.40	0.20	**51.62**	-0.80	**46.62**	33.67	0.11	**72.58**	-0.89	**67.58**
Ni	20	85.80	4.29		3.29		74.77	3.74		2.74	
Cu	1500	270.47	0.18		-0.82		250.00	0.17		-0.83	
Zn	15000	135.98	0.01		-0.99		128.03	0.01		-0.99	
Cd	3	140.84	46.95		45.95		205.67	68.56		67.56	
S14											
Fe	300	77.00	0.26	**55.27**	-0.74	**50.27**	55.27	0.18	**50.75**	-0.82	**45.75**
Ni	20	87.57	4.38		3.38		72.83	3.64		2.64	
Cu	1500	282.80	0.19		-0.81		281.30	0.19		-0.81	
Zn	15000	181.58	0.01		-0.99		171.63	0.01		-0.99	
Cd	3	151.30	50.43		49.43		140.17	46.72		45.72	

nearly similar to those in the main channel. For Ni, earlier studies reported 7–10 μg/L (Singh et al., 2005), 8–105 μg/L (Gaur et al., 2005), and 30–69 μg/L (Gupta et al., 2014). However, in our study, Ni ranged from 10–88 μg/L (pre-monsoon) and 17–81 μg/L (post-monsoon). Ni concentrations are lowest near the headwaters (S1–S3) and increase sharply downstream, reaching to about 80 μg/L (Fig. 2b). Both seasons show a similar trend, but pre-monsoon Ni values are generally higher, likely due to lower water discharge and higher evaporation before the monsoon.

Cu concentrations in Lucknow water varied from 1–4 μg/L (Singh et al., 2005) and 0–35 μg/L (Gaur et al., 2005). Gupta et al. (2014) reported 14–42 μg/L Cu at Lucknow while, Singh et al. (2010) found 11–80 μg/L Cu in Jaunpur. In our data of 2022, Cu levels were much higher, ranging from 26–299 μg/L (pre-monsoon) and 29–297 μg/L (post-monsoon). Cu concentrations gradually increase downstream, reaching the highest level in the Sai tributary (~250 μg/L) (Fig. 2c). Post-monsoon Cu values are slightly lower, reflecting dilution by rainfall. Zn concentrations were

14–29 μg/L (Singh et al., 2005), 30–91 μg/L (Gaur et al., 2005), and 56–74 μg/L (Gupta et al., 2014). In 2022, they were broader, ranging from 2–182 μg/L (pre-monsoon) and 3–172 μg/L (post-monsoon). Zn also shows a gradual rise from S1 to S9 (up to ~180 μg/L) (Fig. 2d). The tributaries have similar or slightly lower Zn levels, except the Sai tributary, which remains relatively high. Zn concentrations vary little between the two seasons.

Cd showed exceptionally high levels (30.9–151.3 μg/L) in 2022, far above values reported earlier. It was below detection limits in Gaur et al., (2005) and 0.1–0.5 μg/L in Singh et al., (2005); both studies were done in Lucknow. However, elevated Cd levels were also noted in later studies: 40–96 μg/L at Jaunpur (Singh et al., 2010), 13–55 μg/L (Gupta et al., 2014) and 50–54 μg/L (Khan et al., 2020, 2021) in Lucknow. All these suggest increasing levels of heavy metal pollution for elements like Ni, Cu, Zn and Pb with time in the Gomati and its tributaries. Cd exhibits a steady downstream increase from ~20 μg/L to more than 140 μg/L, with slightly lower values after the monsoon, again suggesting dilution by rainwater (Fig. 2e). The clear downstream rise in Cd indicates continuous accumulation of contaminants along the river.

Based on classification and distribution using MI, C_d, HPI, and NPI indices, the overall water quality in the Gomati and its tributaries is found to be extremely poor. Table S3 summarizes the water quality of the sampling locations based on various pollution indices. The spatial trend (Fig. 3) confirmed a progressive decline in water quality downstream, consistent across all indices. MI, with all values >6 during both the pre- and post-monsoon seasons fall under *seriously affected* (Class VI) category. C_d values all >3, classifying the sites as *highly polluted*. HPI values exceeded 100 at all sites, increasing from upstream to downstream, classifying the entire river stretch as *critically polluted*. NPI results also categorized the river as *severely polluted* (Class VI). Thus, the Gomati River shows a consistent deterioration of water quality from upstream (S1) to downstream (S9). The combined results of MI, Cd, HPI, and NPI classify the river and its tributaries as severely to critically polluted. The declining pattern of water quality along the river matches the trend of increasing Cd pollution suggesting Cd concentrations in river are at critical values. All the indices showed higher contamination in the river, however such contamination affects are severe in the midstream tributaries like Kathna, Sarayan, and Sai (especially at S13 in Pratapgarh during the post-monsoon) and minimal in the Gomati main channel as concentrations from tributaries get diluted downstream after merging with the river.

Pearson correlation analyses indicate strong associations among metals (Table 3) and suggest that these metals likely originate from common sources or exhibit similar chemical behavior, particularly Cd, Cu, and Ni. The post-monsoon data suggest towards pollutant remobilization due to runoff. Additionally, all metals show negative to negligible correlations with pH in both seasons, indicating that metal concentrations are either unaffected or tend to increase as the water becomes more acidic. This may be due to release of heavy metals by sediments into water as acidity increases. However, the Caboi's diagram suggest most of our samples fell into the "near neutral-extreme metal" category suggesting although our samples are close to neutral in pH (6.5–8.5) but the water carries very high metal loads. This reflects severe contamination, as neutral pH typically favors better water quality but here high metal concentrations override the buffering capacity of the system. None of the samples fall in other fields, suggesting that metal enrichment is the primary issue, not acidification. This pattern implies that the Gomati River and its tributaries are under serious heavy metal stress. Thus, Caboi's Diagram discards the possibility of release of metals by natural geochemical acidification processes, rather it suggests to be driven by anthropogenic inputs (Fig. 5). HCA during both the seasons grouped the heavy metals into two clusters: Cluster 1 including Zn, Cd, Fe, Ni suggesting a common source to these and Cluster 2 having Cu alone.

Table 5: Estimation of Heavy metal pollution index (HPI) and Nemerow pollution index (NPI) for different sampling sites of the Gomati River main channel and tributaries.

				Pre-Monsoon						**Post-Monsoon**					
Samples/ Symbols	**Standard Permissible Limit (Si) in ppb**	**Ideal Value (Ii) in ppb**	**Unit Weight Value (Wi)**	**Monitor Value (Mi) in ppb**	**Qi= |Mi-Ii|/ (Si-Ii)*100**	**WiQi**	**HPI = ΣWiQi/ ΣWi**	**Pi**	**NPI**	**Monitor Value (Mi) in ppb**	**Qi= |Mi-Ii|/ (Si-Ii)*100**	**WiQi**	**HPI = ΣWiQi/ ΣWi**	**Pi**	**NPI**
S1															
Fe	300	0	0.00	86.60	28.87	0.10	**1457.2**	0.29	**8.4**	76.91	25.64	0.09	**1282.1**	0.26	**7.5**
Ni	70	20	0.01	37.07	34.13	0.49		1.85		20.00	0.00	0.00		1.00	
Cu	1500	50	0.00	0.00	3.45	0.00		0.00		0.00	3.45	0.00		0.00	
Zn	15000	5000	0.00	13.17	49.87	0.00		0.00		13.73	49.86	0.00		0.00	
Cd	5	3	0.20	34.75	1587.56	317.51		11.58		30.99	1399.33	279.87		10.33	
S2															
Fe	300	0	0.00	28.50	9.50	0.03	**1825.4**	0.10	**10.4**	27.90	9.30	0.03	**1684.5**	0.09	
Ni	70	20	0.01	49.70	59.40	0.85		2.49		29.93	19.87	0.28		1.50	
Cu	1500	50	0.00	0.00	3.45	0.00		0.00		0.00	3.45	0.00		0.00	
Zn	15000	5000	0.00	2.03	49.98	0.00		0.00		3.06	49.97	0.00		0.00	
Cd	5	3	0.20	42.76	1987.97	397.59		14.25		39.75	1837.50	367.50		13.25	**9.6**
S3															
Fe	300	0	0.00	34.08	11.36	0.04	**2139.1**	0.11	**12.0**	38.56	12.85	0.04	**1525.7**	0.13	**8.8**
Ni	70	20	0.01	19.26	1.49	0.02		0.96		33.95	27.90	0.40		1.70	
Cu	1500	50	0.00	0.00	3.45	0.00		0.00		0.00	3.45	0.00		0.00	
Zn	15000	5000	0.00	10.77	49.89	0.00		0.00		12.81	49.87	0.00		0.00	
Cd	5	3	0.20	49.69	2334.48	466.90		16.56		36.27	1663.50	332.70		12.09	
S4															
Fe	300	0	0.00	28.60	9.53	0.03	**2905.6**	0.10	**16.0**	35.63	11.88	0.04	**1721.0**	0.12	**9.8**
Ni	70	20	0.01	10.58	18.85	0.27		0.53		17.73	4.53	0.06		0.89	
Cu	1500	50	0.00	29.01	1.45	0.00		0.02		29.47	1.42	0.00		0.02	
Zn	15000	5000	0.00	71.33	49.29	0.00		0.00		56.80	49.43	0.00		0.00	
Cd	5	3	0.20	66.40	3169.83	633.97		22.13		40.57	1878.33	375.67		13.52	

S5															
Fe	300	0	0.00	37.17	12.39	0.04	**3106.6**	0.12	**17.1**	44.13	14.71	0.05	**3024.5**	0.15	
Ni	70	20	0.01	28.51	17.03	0.24		1.43		19.50	1.00	0.01		0.98	
Cu	1500	50	0.00	74.37	1.68	0.00		0.05		74.03	1.66	0.00		0.05	
Zn	15000	5000	0.00	53.67	49.46	0.00		0.00		52.14	49.48	0.00		0.00	
Cd	5	3	0.20	70.79	3389.33	677.87		23.60		69.03	3301.67	660.33		23.01	**16.6**
S6															
Fe	300	0	0.00	45.52	15.17	0.05	**3594.2**	0.15	**19.6**	51.88	17.29	0.06	**3646.2**	0.17	**19.9**
Ni	70	20	0.01	39.78	39.56	0.57		1.99		27.63	15.27	0.22		1.38	
Cu	1500	50	0.00	26.94	1.59	0.00		0.02		0.00	3.45	0.00		0.00	
Zn	15000	5000	0.00	108.37	48.92	0.00		0.01		22.25	49.78	0.00		0.00	
Cd	5	3	0.20	81.40	3919.83	783.97		27.13		82.59	3979.33	795.87		27.53	
S7															
Fe	300	0	0.00	64.26	21.42	0.07	**4433.0**	0.21	**24.1**	46.39	15.46	0.05	**4063.7**	0.15	**22.1**
Ni	70	20	0.01	67.10	94.20	1.35		3.36		52.60	65.20	0.93		2.63	
Cu	1500	50	0.00	86.93	2.55	0.00		0.06		83.40	2.30	0.00		0.06	
Zn	15000	5000	0.00	101.23	48.99	0.00		0.01		21.77	49.78	0.00		0.00	
Cd	5	3	0.20	99.63	4831.33	966.27		33.21		91.63	4431.67	886.33		30.54	
S8															
Fe	300	0	0.00	54.43	18.14	0.06	**4868.4**	0.18	**26.3**	57.27	19.09	0.06	**4375.9**	0.19	
Ni	70	20	0.01	74.37	108.73	1.55		3.72		69.20	98.40	1.41		3.46	
Cu	1500	50	0.00	164.60	7.90	0.01		0.11		163.00	7.79	0.01		0.11	
Zn	15000	5000	0.00	102.56	48.97	0.00		0.01		102.00	48.98	0.00		0.01	
Cd	5	3	0.20	109.11	5305.57	1061.11		36.37		98.40	4770.00	954.00		32.80	**23.8**
S9															
Fe	300	0	0.00	49.52	16.51	0.06	**5305.2**	0.17	**28.6**	58.08	19.36	0.06	**5056.8**	0.19	**27.3**
Ni	70	20	0.01	73.76	107.52	1.54		3.69		58.03	76.07	1.09		2.90	
Cu	1500	50	0.00	199.62	10.32	0.01		0.13		0.00	3.45	0.00		0.00	
Zn	15000	5000	0.00	114.60	48.85	0.00		0.01		108.68	48.91	0.00		0.01	
Cd	5	3	0.20	118.65	5782.42	1156.48		39.55		113.30	5515.00	1103.00		37.77	

S10															
Fe	300	0	0.00	56.23	18.74	0.06	**5405.7**	0.19	**29.2**	56.41	18.80	0.06	**4955.5**	0.19	**26.8**
Ni	70	20	0.01	79.03	118.07	1.69		3.95		65.90	91.80	1.31		3.30	
Cu	1500	50	0.00	215.50	11.41	0.01		0.14		205.90	10.75	0.01		0.14	
Zn	15000	5000	0.00	144.29	48.56	0.00		0.01		137.80	48.62	0.00		0.01	
Cd	5	3	0.20	120.83	5891.33	1178.27		40.28		111.07	5403.33	1080.67		37.02	
S11															
Fe	300	0	0.00	47.27	15.76	0.05	**5778.8**	0.16	**31.1**	35.57	11.86	0.04	**5359.8**	0.12	
Ni	70	20	0.01	84.06	128.12	1.83		4.20		76.30	112.60	1.61		3.82	
Cu	1500	50	0.00	214.87	11.37	0.01		0.14		246.00	13.52	0.01		0.16	**28.9**
Zn	15000	5000	0.00	138.67	48.61	0.00		0.01		127.63	48.72	0.00		0.01	
Cd	5	3	0.20	128.96	6297.90	1259.58		42.99		119.87	5843.33	1168.67		39.96	
S12															
Fe	300	0	0.00	63.27	21.09	0.07	**6066.5**	0.21	**32.6**	63.50	21.17	0.07	**5716.3**	0.21	
Ni	70	20	0.01	84.73	129.47	1.85		4.24		81.13	122.27	1.75		4.06	
Cu	1500	50	0.00	299.33	17.20	0.01		0.20		297.33	17.06	0.01		0.20	**30.8**
Zn	15000	5000	0.00	128.88	48.71	0.00		0.01		119.43	48.81	0.00		0.01	
Cd	5	3	0.20	135.23	6611.70	1322.34		45.08		127.63	6231.67	1246.33		42.54	
S13															
Fe	300	0	0.00	59.40	19.80	0.07	**6323.4**	0.20	**34.0**	33.67	11.22	0.04	**5869.5**	0.11	
Ni	70	20	0.01	85.80	131.60	1.88		4.29		74.77	109.53	1.56		3.74	
Cu	1500	50	0.00	270.47	15.20	0.01		0.18		250.00	13.79	0.01		0.17	**49.6**
Zn	15000	5000	0.00	135.98	48.64	0.00		0.01		128.03	48.72	0.00		0.01	
Cd	5	3	0.20	140.84	6892.00	1378.40		46.95		205.67	6400.00	1280.00		68.56	
S14															
Fe	300	0	0.00	77.00	25.67	0.09	**6803.0**	0.26	**36.5**	55.27	18.42	0.06	**6289.2**	0.18	
Ni	70	20	0.01	87.57	135.13	1.93		4.38		72.83	105.67	1.51		3.64	
Cu	1500	50	0.00	282.80	16.06	0.01		0.19		281.30	15.95	0.01		0.19	**33.8**
Zn	15000	5000	0.00	181.58	48.18	0.00		0.01		171.63	48.28	0.00		0.01	
Cd	5	3	0.20	151.30	7415.02	1483.00		50.43		140.17	6858.33	1371.67		46.72	

* For NPI calculation Maximum Allowable conc. (MAC) is same as given in Table 3.

Table 6: The level of heavy metal pollution at different sampling sites of the Gomati River main channel and tributaries based on the estimated MI, C_d, HPI, NPI values.

Sampling sites	Seasons	MI	Rating of water quality	Cd	Rating of water quality	HPI	Rating of water quality	NPI	Rating of water quality
S1	Pre- Monsoon	13.7	Seriously affected	8.7	High pollution	1457	Critically polluted	8.4	Seriously polluted
	Post- Monsoon	11.6	Seriously affected	6.6	High pollution	1282	Critically polluted	7.5	Seriously polluted
S2	Pre- Monsoon	16.8	Seriously affected	11.8	High pollution	1825	Critically polluted	10.4	Seriously polluted
	Post- Monsoon	14.8	Seriously affected	9.8	High pollution	1685	Critically polluted	9.6	Seriously polluted
S3	Pre- Monsoon	17.6	Seriously affected	12.6	High pollution	2139	Critically polluted	12.0	Seriously polluted
	Post- Monsoon	13.9	Seriously affected	8.9	High pollution	1527	Critically polluted	8.8	Seriously polluted
S4	Pre- Monsoon	22.8	Seriously affected	17.8	High pollution	2906	Critically polluted	16.0	Seriously polluted
	Post- Monsoon	14.6	Seriously affected	9.6	High pollution	1721	Critically polluted	9.8	Seriously polluted
S5	Pre- Monsoon	25.2	Seriously affected	20.2	High pollution	3107	Critically polluted	17.1	Seriously polluted
	Post- Monsoon	24.2	Seriously affected	19.2	High pollution	3024	Critically polluted	16.6	Seriously polluted
S6	Pre- Monsoon	29.3	Seriously affected	24.3	High pollution	3594	Critically polluted	19.6	Seriously polluted
	Post- Monsoon	29.1	Seriously affected	24.1	High pollution	3646	Critically polluted	19.9	Seriously polluted
S7	Pre- Monsoon	36.8	Seriously affected	31.8	High pollution	4433	Critically polluted	24.1	Seriously polluted
	Post- Monsoon	33.4	Seriously affected	28.4	High pollution	4064	Critically polluted	22.1	Seriously polluted
S8	Pre- Monsoon	40.4	Seriously affected	35.4	High pollution	4868	Critically polluted	26.3	Seriously polluted
	Post- Monsoon	36.6	Seriously affected	31.6	High pollution	4376	Critically polluted	23.8	Seriously polluted
S9	Pre- Monsoon	43.5	Seriously affected	38.5	High pollution	5305	Critically polluted	28.6	Seriously polluted
	Post- Monsoon	41.0	Seriously affected	36.0	High pollution	5057	Critically polluted	27.3	Seriously polluted
S10	Pre- Monsoon	44.6	Seriously affected	39.6	High pollution	5406	Critically polluted	29.2	Seriously polluted
	Post- Monsoon	40.7	Seriously affected	35.7	High pollution	4956	Critically polluted	26.8	Seriously polluted
S11	Pre- Monsoon	47.5	Seriously affected	42.5	High pollution	5779	Critically polluted	31.1	Seriously polluted
	Post- Monsoon	44.1	Seriously affected	39.1	High pollution	5360	Critically polluted	28.9	Seriously polluted
S12	Pre- Monsoon	49.7	Seriously affected	44.7	High pollution	6067	Critically polluted	32.6	Seriously polluted
	Post- Monsoon	47.0	Seriously affected	42.0	High pollution	5716	Critically polluted	30.8	Seriously polluted
S13	Pre- Monsoon	51.6	Seriously affected	46.6	High pollution	6323	Critically polluted	34.0	Seriously polluted
	Post- Monsoon	72.6	Seriously affected	67.6	High pollution	5869	Critically polluted	49.6	Seriously polluted
S14	Pre- Monsoon	55.3	Seriously affected	50.3	High pollution	6803	Critically polluted	36.5	Seriously polluted
	Post-Monsoon	50.7	Seriously affected	45.7	High pollution	6289	Critically polluted	33.8	Seriously polluted

HCA on the Gomati River sampling sites group them into three main clusters (Fig. 4a&b). During the pre-monsoon season, Cluster 1 (S1–S7) represents upstream sites with better water quality and minimal human impact. Cluster 2 (S12–S14) includes sites on the Sai tributary, which has independent pollution sources. Cluster 3 (S8–S11) covers downstream and tributary sites showing higher pollution. The downstream sites S8 and S9 are appeared to be influenced by upstream tributaries and midstream pollutions whereas tributaries Kathna (S10) and Sarayan (S11) having their own sub-basins possibly have high pollution inputs from localized sources (urban/industrial) similar to Sai. This indicates a clear separation between cleaner upstream waters (S1–S7) and polluted downstream main channel (S8–S9) and tributaries (S10–S14). In the post-monsoon season (Fig. 4b), clustering patterns change due to rainfall and runoff. Cluster 1 (S8–S14) includes downstream sites of main channel and tributary sites Kathna (S10), Sarayan (S11) and Sai (S12–S14) that show similar water quality because of mixing and dilution during high flow. Cluster 2 (S1–S4, S7) and Cluster 3 (S5–S6) represent upstream and midstream sites with moderate pollution, reflecting the dilution effect of monsoonal discharge. Therefore, the post-monsoon results suggest reduced variability and greater homogenization of water quality across the river.

Overall, the pre-monsoon shows sharper separation between upstream (less polluted) and downstream/tributary sites (more polluted), while post-monsoon clusters are broader, reflecting mixing and dilution. Downstream sites of Gomati main channel (S8, S9) and tributary-influenced sites (S10, S11 and S12–S14) consistently cluster together, highlighting them as critical zones of heavy metal pollution. Heavy rainfall and runoff during monsoons reduce variability across sites, but pollution from tributaries (especially Kathna, Sarayan, Sai) still dominates. These seasonal shifts suggest that monsoonal runoff and dilution influence water quality similarity across sites, reducing variability in downstream locations while highlighting pollution hotspots in certain tributary-influenced regions.

The increasing concentrations of all metals downstream also suggest towards growing human influence on water quality. Human activities contribute significantly to heavy metal pollution through agricultural runoff, industrial effluents, and domestic wastewater. Since there is almost no mining or large-scale excavation in the Gomati basin, such sources can be avoided. However, most of the basin is agricultural land and therefore use of fertilizers, pesticides, and fungicides that often contain trace amounts of Fe, Cu, Cd, Zn, and Ni cannot be neglected. These pollutants reach rivers and groundwater through runoff from fields, particularly during the monsoons. Industrial sources such as smelting operations release Zn and Cd, while iron and steel plants and metal-processing industries discharge effluents rich in Fe, Ni, and Zn. Metallurgical, refractory, and leather industries may release Cu into the environment through wastewater. Ni, widely used in batteries and electroplating, can enter the river from improper disposal of industrial and battery waste and e-waste dismantling. Electroplating, paint, pigment, and tannery industries are also common sources of Ni and Cd contamination. Domestic sewage and wastewater from urban areas are another major source of Cu, Zn, Ni, and Cd pollution, as they are often released untreated into the river. Many household products and detergents also contain Ni and other metals. Rainwater runoff from urban and industrial areas carries metals from roads, construction sites, and drains into the river. Leachate from landfills containing metallic waste can further pollute both surface and groundwater. Atmospheric emissions from industries and vehicles also deposit Fe, Zn, Cu, and Cd onto land and water surfaces through rainfall. There are many other industries like sugar, rice, oil and flour mills in the Gomati basin but that are not likely seemed to be responsible for heavy metal pollution.

Previous studies around Lucknow have also confirmed the presence of heavy metals in the sediments and water of the Gomati River (Singh et al., 1997; Gaur et al., 2005; Singh et al., 2005; Lohani et al., 2008; Neha et al. 2017; Gupta et al., 2014; Khan et al., 2020, 2021). Major sources of this pollution include the Kukrail, Hyder canal, and several smaller drains that carry untreated or partially treated municipal wastewater, urban effluents, and agricultural runoff. The present data show that pollution increases steadily downstream in the Gomati River and its tributaries. Metal concentrations are slightly higher during the pre-monsoon period due to low flow and limited dilution. Tributaries show higher metal concentrations, suggesting they have their own pollution sources, though these impacts are less visible in the main river channel. Among them the Sai (S12–S14) has the highest contamination, likely from urban and industrial discharges from Unnao, Rae Bareli, and Pratapgarh. Fe levels in the samples are within or below the acceptable limits set by BIS (2012), so it is not a major concern. However, Ni concentrations increase after site S4 and exceed safe limits at downstream locations (S8 & S9). Likely sources of Ni include iron and steel industries, electroplating, paint and pigment manufacturing, tanneries, battery waste, and e-waste dismantling.

Cu is absent at upstream sites, indicating little natural input. Its concentration rises sharply after the Sarayan River joins the Gomati main channel (before S4) and continues to increase downstream, mainly due to mixed agricultural,

industrial, and domestic pollution from urban centers such as Sitapur, Lucknow, Sultanpur, and Jaunpur. Zn levels also remain high after site S3, likely due to contributions from sewage, vehicle emissions, agricultural runoff, and galvanization activities. Cd shows a steady rise from upstream (S1) to downstream (S9), with concentrations (in 2022) higher than previously reported. Major Cd sources include metal plating, fertilizers, Ni–Cd batteries, plastic and textile industries, sewage effluents, and pigment production. It can also enter water from Zn extraction, landfill leachates, and corroded galvanized pipes.

High levels of Ni and Cd at several sites indicate possible ecological and health risks, especially in the middle and lower parts of the river. Cd, one of the most toxic metals after Hg, naturally occurs in small amounts in soil and sediments (0.15–0.2 mg/kg). In polluted rivers, Cd levels in water are usually very low (0.10–0.50 μg/L) and sometimes undetectable. It is mostly found as inorganic compounds (like carbonates, hydroxides, chlorides, or sulphates) or bound to organic matter. According to the BIS, the safe limit of Cd in drinking water is 3 μg/L with no relaxation allowed. Long-term exposure, even at low levels, can cause serious health problems such as kidney damage, bone weakness (osteoporosis), high blood pressure, and cardiovascular or lung diseases. Cd mainly enters the body through the digestive system and accumulates in the liver, kidneys, and bones for up to 10–20 years (Rasin, et al., 2025). Inhalation or acute exposure can cause nausea, vomiting, chest pain, and breathing problems. A severe example of Cd poisoning was the Itai-Itai disease in Japan. Ni contamination is also concerning due to its potential to accumulate in aquatic organisms, affecting fish health and ecosystems. In humans, ingestion of Ni-contaminated water or food can lead to allergies, kidney and heart problems, and even cancer.

Cd pollution hotspots with increased levels of Cd above the acceptable limits have also been reported by Central Water Commision (2019) in the Ganga, Kopili, Rapti, Tungabhadra, and Yamuna rivers with the highest concentration (70.51 μg/L) recorded in the Sabarmati River out of total of Indian rivers 2,908 river water samples collected and analyzed between May 2014 and April 2018. The cities and towns along the direct pathway of the Gomati main channel and tributaries are densely populated; some of these are well-developed and industrialized, with many small –scale electronic based industries. The illegal dismantling of e-waste is now common everywhere, often involving open-air burning, acid treatment, or other crude methods to recover valuable parts. Such practices release toxic metals into the environment such as Cd from cathode ray tubes and chips, and Cd from broken glass. These can leach into water, making it acidic, especially in landfill sites. Open-air burning also releases toxic by-products into the atmosphere, which later spread locally and globally (Sivakumar et al., 2011; Ramachandra and Saira, 2004). In India, the informal sector handles nearly 90% of E-waste. Rag pickers collect scraps from offices and households and extract metals without proper safety measures. Since most workers are unskilled and lack knowledge or technology, recycling and disposal are done improperly. This highlights the urgent need for a structured E-waste management system. Improved technologies, formal recycling methods, awareness programs, and environmental education could help reduce pollution and promote safer handling of E-waste. Strict regulations and advanced treatment of industrial wastewater are essential to reduce heavy metal pollution. Upgrading sewage treatment plants and drainage systems can help limit contamination from urban sources. Encouraging careful use of fertilizers and pesticides will also reduce agricultural runoff. Regular monitoring of heavy metal levels in the Gomati River and its tributaries, along with strict enforcement of environmental laws, is necessary to protect water quality.

5. Conclusion

The present study highlights a serious and progressive deterioration in the water quality of the Gomati River and its tributaries, primarily due to heavy metal pollution. A comparison with earlier studies indicates a substantial rise in the

concentrations of Ni, Cu, Zn, and Cd in 2022, while Fe levels have declined and remain within acceptable limits. The consistent downstream increase in heavy metal concentrations, especially for Cd and Ni, points to growing anthropogenic pressure from industrial, agricultural, and domestic sources. Tributaries such as Kathna, Sarayan, and particularly Sai have emerged as major contributors to this contamination, reflecting inputs from urban and industrial regions like Sitapur, Lucknow, Rae Bareli, Sultanpur, and Jaunpur. Multivariate analyses (MI, Cd, HPI, and NPI) classify the river as 'severely' to 'critically polluted', with water quality declining steadily downstream. Correlation and cluster analyses reveal strong inter-metal relationships, suggesting common anthropogenic origins, while Caboi's diagram indicates high metal enrichment under near-neutral pH conditions, ruling out natural geochemical causes. Seasonal variations show that pre-monsoon concentrations are higher due to low flow and evaporation, whereas post-monsoon dilution temporarily reduces contamination but does not eliminate it. The elevated levels of Cd and Ni at several sites raise significant ecological and public health concerns. The unregulated disposal of e-waste, industrial effluents, and agrochemical runoff appear to be the major sources contributing to the contamination of the Gomati basin. To restore the ecological health of the Gomati River, urgent management actions are required including stricter enforcement of industrial discharge standards, effective operation and expansion of sewage treatment facilities, safe e-waste recycling, and sustainable agricultural practices to minimize heavy metal inputs. Without timely intervention, the continued accumulation of heavy metals could further degrade water quality, harm aquatic ecosystems, and pose serious risks to the health and livelihoods of communities dependent on the Gomati River system.

6. Limitation and future scope the study

Although this study provides valuable insights into the spatial and seasonal variations of heavy metal contamination in the Gomati River and its tributaries, certain limitations should be acknowledged. First, the sampling was limited to two seasonal periods (pre- and post-monsoon) within a single year (2022), which may not fully represent long-term temporal variations or inter-annual trends influenced by climatic or anthropogenic changes. Secondly, while the study focused on dissolved heavy metals in water, it did not include sediment or biota analysis, which could have provided a more comprehensive understanding of heavy metal accumulation, bioavailability, and trophic transfer. The study also relied primarily on conventional pollution indices and statistical tools; the inclusion of advanced geochemical modeling, isotopic tracing, or machine-learning-based source apportionment could further refine the interpretation of pollution sources and dynamics. Moreover, spatial resolution was constrained by accessibility and logistical limitations, and some minor tributaries or point sources may have been overlooked. Future research should expand temporal and spatial coverage to include multi-year continuous monitoring across dry and wet seasons to capture dynamic changes in heavy metal inputs and transport mechanisms. Integrating sediment, soil, and biological monitoring will help assess metal accumulation and potential ecological and human health risks. The use of remote sensing and GIS-based modeling could enhance spatial visualization of pollution hotspots and aid management planning. Isotopic fingerprinting and speciation studies are recommended to distinguish between natural and anthropogenic metal sources. Additionally, long-term monitoring programs and ecological risk assessment frameworks should be established to evaluate the effectiveness of pollution control measures. Collaborative efforts involving government agencies, academic institutions, and local stakeholders will be vital for developing sustainable river management strategies. Such integrative approaches can contribute significantly to restoring the ecological health and water quality of the Gomati River system.

Acknowledgement

The authors sincerely thank Anamika Yadav, Gautam Vishwakarma, and Anand Rao for their

assistance in sample collection during fieldwork. We are also grateful to the staff of the research laboratory at Hindalco Alumina Power Plant, Sonbhadra (U.P.), for providing analytical facilities and technical support throughout this study. This research did not receive any financial support or funding from any organization.

References

1. **Abeysingha NS, Islam A, Singh M** (2020) Assessment of climate change impact on flow regimes over the Gomati River basin under IPCC AR5 climate change scenarios. *J Water Clim Change* 11(1):303–326. https ://doi.org/10.2166/wcc.2018.039.
2. **Ahamad MI, Yao Z, Ren L, Zhang C, Li T, Lu H, Mehmood MS, Rehman A, Adil M, Lu S and Feng W** (2024) Impact of heavy metals on aquatic life and human health: a case study of River Ravi Pakistan. *Front. Mar. Sci.* 11:1374835. **doi: 10.3389/fmars.2024.1374835**
3. **Ahmad MK, Islam S, Rahman S, Haque MR, Islam MM** (2010) Heavy metals in water, sediment and some fishes of Buriganga River, Bangladesh. Int J Environ Res 4(2):321–332. **https ://doi.org/10.22059/ijer.2010.24**
4. **Ahmad S, Khurshid S** (2019) Hydrogeochemical assessment of groundwater quality in parts of the Hindon River basin, Ghaziabad, India: implications for domestic and irrigation purposes. SN Appl Sci 1:151. **https ://doi.org/10.1007/s4245 2-019-0161-9**
5. **Akoto O, Bruce TN, Darko G** (2008) Heavy metals pollution profiles in streams serving the Owabi reservoir. *Afr J Environ Sci Technol* 2(11):354–359.
7. **Amadi AN** (2011) Assessing the Effects of Aladimma dumpsite on soil and groundwater using water quality index and factor analysis. *Aust J Basic Appl Sci* 5(11):763–770
8. **APHA**. (2017). Standard methods for the examination of water and wastewater (23rd ed.). American Public Health Association.
9. **Babiker IS, Mohamed AA, Hiyama T** (2007) Assessing groundwater quality using GIS. Water Resour Manag 21:699–715. **https ://doi.org/10.1007/s1126 9-006-9059-6**
10. **BIS**. (2012). Drinking Water Specification, Second Revision IS:10500: 2012. Bureau of Indian Standards, New Delhi, India.
11. **Caboi, R., Cidu, R., Fanfani, L., Lattanzi, P., & Zuddas, P.** (1999). Environmental mineralogy and geochemistry of the abandoned Pb–Zn Montevecchio-Ingurtosu mining district, Sardinia, Italy. *Chron Rech Miniere*, 534, 21–28.
12. **Caeiro, S., Costa, M.H., Ramos, T.B., Fernandes, F., Silveira, N., Coimbra, A., Medeiros, G. and Painho, M.**, 2005. Assessing heavy metal contamination in Sado Estuary sediment: an index analysis approach. *Ecological indicators*, 5(2), pp.151-169.
13. **Djordjević L, Živković N, Živković L, Djordjević A** (2012) Assessment of heavy metals pollution in sediments of the Korbevačka river in south eastern Serbia. Soil Sediment Contam 21:889–900. **https ://doi.org/10.1080/15320 383.2012.69911 0**
14. **Dutta V, Srivastava RK, Yunus M, Ahmed S, Pathak VV, Rai L, Prasad N** (2011) Restoration plan of Gomati River with designated best use classification of surface water quality based on river expedition, monitoring and quality assessment. *Earth Science India*. 4(III):80–104.
15. **Dutta V, Urvashi K, Sharma U** (2015) Assessment of humaninduced impacts on hydrological regime of Gomati river basin, India. *Manag Environ Qual Int J* 26(5):631–649. **https ://doi.org/10.1108/MEQ-11-2014-0160**
16. **Edet AE, Offiong OE** (2002) Evaluation of water quality pollution indices for heavy metal contamination monitoring. A study case from Akpabuyo-Odukpani area, Lower Cross River Basin (southeastern Nigeria). Geo J 57:295–304

17. **Ficklin, D., Plumee, G., Smith, K., & McHugh, J.** (1992). Geochemical classification of mine drainages and natural drainages in mineralized areas. Water–Rock Interact, 1, 381–384).

18. **Gaur VK, Gupta SK, Pandey SD, Gopal K, Misra V** (2005) Distribution of heavy metals in sediment and water of river Gomati. Environ Monit Assess 102:419–433. **https ://doi.org/10.1007/s10661-005-6395-6**

19. **Goel P**. (2018) Identification of the source mineral releasing arsenic in the groundwater of the Indo-Gangetic Plain, India. In: Hussain CM (ed) Handbook of environmental materials management. Springer, Cham, pp 247–283. **https ://doi.org/10.1007/978-3-319-58538 -3_129-1**

20. **Gupta, P.K.,** 2020. Pollution load on Indian soil-water systems and associated health hazards: a review. *Journal of Environmental Engineering*, 146(5), p.03120004.

21. **Gupta KS, Chabukdhara M, Kumar P, Singh J, Bux F** (2014) Evaluation of ecological risk of metal contamination in river Gomati, India: a biomonitoring approach. Ecotoxicol Environ Saf 110:49–55. **https ://doi.org/10.1016/j.ecoen v.2014.08.008**

22. **Gupta LP, Subramanian V** (1994) Environmental geochemistry of the River Gomati: a tributary of the Ganges River. Environ Geol 24:235–243. **https ://doi.org/10.1007/BF007 67084**

23. **Horton RK** (1965) An index number system for rating water quality. *J Water Pollut Control Fed*. 37(3):300–306

24. **Islam, M.S., Han, S., Ahmed, M.K. and Masunaga, S.,** 2014. Assessment of trace metal contamination in water and sediment of some rivers in Bangladesh. *Journal of water and environment technology*, 12(2), pp.109-121.

25. **Khadse GK, Patni PM, Kelkar PS, Devotta S** (2008) Qualitative evaluation of Kanhan river and its tributaries flowing over central Indian plateau. Environ Monitor Assess 147(1–3):83–92. **https ://doi.org/ 10.1007/s1066 1-007-0100-x**

26. **Khan, R., Saxena, A., Shukla, S.** (2020). Evaluation of heavy metal pollution for River Gomati, in parts of Ganga Alluvial Plain, India. *SN Applied Sciences*, 2:1451.

27. **Khan, R., Saxena, A., Shukla, S.** (2021). Assessment of the impact of COVID-19 lockdown on the heavy metal pollution in the River Gomati, Lucknow city, Uttar Pradesh, India. *Environmental Quality Management*. 1–9.

28. **Kumar S, and Singh, IB.** (1978). Sedimentological study of Gomati River sediments, U.P. India – Example of a river in alluvial plain; Senckenberg Merit 10: 145–211.

29. **Kumar R, Kumar V, Sharma A** et al (2019) Assessment of pollution in roadside soils by using multivariate statistical techniques and contamination indices. *SN Appl Sci* 1:842. **https :// doi.org/10.1007/s4245 2-019-0888-3**

30. **Kumari, B. and Awasthi, N.,** 2025. Seasonal variations in physicochemical characteristics of the River Gomati from Pilibhit to Jaunpur District, Uttar Pradesh, India. Discover Water, 5(1), p.95.

31. **Li P, Qian H, Howard KWF, Wu J** (2015) Heavy metal contamination of Yellow River alluvial sediments, northwest China. Environ Earth Sci 73(7):3403–3415. **https://doi.org/10.1007/s12665-014-3628-4**

32. **Li P, Wu J, Qian H, ZhouW** (2016) Distribution, enrichment and sources of tracemetals in the topsoil in the vicinity of a steel wire plant along the Silk Road economic belt, northwest China. ***Environ Earth Sci*** 75(10):909. **https://doi.org/ 10.1007/s12665-016-5719-x**

33. **Liao, J., Chen, J., Ru, X., Chen, J., Wu, H. and Wei, C.,** 2017. Heavy metals in river surface sediments affected with multiple pollution sources, South China: Distribution, enrichment and source apportionment. *Journal of Geochemical Exploration*, 176, pp.9-19.

34. **Lin, Y.C., Chang-Chien, G.P., Chiang, P.C., Chen, W.H. and Lin, Y.C.,** 2013. Multivariate analysis of heavy metal contaminations in seawater and sediments from a heavily industrialized harbor in Southern Taiwan. *Marine pollution bulletin*, 76(1-2), pp.266-275.

35. **Lohani MB, Singh A, Rupainwar CD, Dhar ND** (2008) Seasonal variations of heavy metal contamination in river Gomati of Lucknow city region. *Environ Monit Assess* 147:253–263. https :// ***doi.org/10.1007/s1066 1-007-0117-1***

36. **Maiti, S.K. and Chowdhury, A.,** 2013. Effects of Anthropogenic Pollution on Mangrove Biodiversity: A Review. *Journal of Environmental Protection*, 4, pp.1428-1434.

37. **Mishra S, Kumar A, Shukla P** (2015) Study of water quality in Hindon River using pollution index and environmetrics, India. Desalin Water Treat. **https ://doi.org/10.1080/19443 994.2015.10985 7**0

38. **Mohan SV, Nithila P, Reddy SJ** (1996) Estimation of heavy metal in drinking water and development of heavy metal pollution index. *J Environ Sci Health* A 31(2):283–289. **https ://doi.org/10.1080/10934 52960 93763 57.**

39. **Morillo, J., Usero, J. and Gracia, I.,** 2004. Heavy metal distribution in marine sediments from the southwest coast of Spain. Chemosphere, 55(3), pp.431-442.

40. **Nemerow, N.L.,** 1991. Stream, lake, estuary, and ocean pollution. John Wiley & Sons, New York, USA (1991)

41. **Neha, Kumar, D., Shukla, P., Kumar, S., Bauddh, K., Tiwari, J., Dwivedi, N., Barman, S.C., Singh, D.P. and Kumar, N.,** 2017. Metal distribution in the sediments, water and naturally occurring macrophytes in the river Gomati, Lucknow, Uttar Pradesh, India. Current Science, pp.1578-1585.

42. **Nicolau, R., Galera-Cunha, A. and Lucas, Y.,** 2006. Transfer of nutrients and labile metals from the continent to the sea by a small Mediterranean river. *Chemosphere*, 63(3), pp.469-476.

43. **Nies, D.H.,** 1999. Microbial heavy-metal resistance. Applied microbiology and biotechnology, 51(6), pp.730-750.

44. **Paramasivam, K., Ramasamy, V. and Suresh, G.,** 2015. Impact of sediment characteristics on the heavy metal concentration and their ecological risk level of surface sediments of Vaigai river, Tamilnadu, India. *Spectrochimica Acta Part A: Molecular and Biomolecular Spectroscopy*, 137, pp.397-407.Prasad B,

45. **Bose JM** (2001) Evaluation of heavy metal pollution index for surface and spring water near a limestone mining area of the lower Himalayas. *Environ Geol*. 41:183–188

46. **Singh, P. and Kumari, B** (2023). A review on toxicity of major heavy metals. WJERT. 9, 8(203-214).

47. **Quamar F, Ali NS, Morthekai P, Singh KV** (2017) Confocal (CLSM) and light (LM) photomicrographs of different plant pollen taxa from Lucknow, India: implications of pollen morphology for systematics, phylogeny and preservation. Rev Palaeobot Palynol. **https ://doi.org/10.1016/j.revpalbo.2017.09.005**

48. **Rai, S., Gupta, S. and Mittal, P.C.,** 2015. Dietary intakes and health risk of toxic and essential heavy metals through the food chain in agricultural, industrial, and coal mining areas of northern India. *Human and Ecological Risk Assessment: An International Journal*, 21(4), pp.913-933.

49. **Rai PK, Mishra A, Tripathi BD** (2010) Heavy metal and microbial pollution of the River Ganga: A case study of water quality at Varanasi. Aquat Ecosyst Health Manage 13:4:(352–361). **https ://doi.org/10.1080/14634 988.2010.52873 9**

50. **Ramachandra, T.V., Saira Varghese, K.** (2004). Environmentally sound option for e-waste management. http://www.ces.

iisc.ernet.in/energy/paper/ ewaste/ewaste.html#5.

51. **Rasin, P., Ashwathi, A.V., Basheer, S.M., Haribabu, J., Santibanez, J.F., Garrote, C.A., Arulraj, A. and Mangalaraja, R.V.,** 2025. Exposure to cadmium and its impacts on human health: A short review. *Journal of Hazardous Materials Advances*, p.100608.

52. **Schumm SA, Dumont JF, Holbrook JM** (2000) Active tectonics and alluvial rivers. Cambridge University Press, Cambridge. **https://doi.org/10.1002/jqs.698**

53. **Saha, S.B., Mitra, A., Bhattacharyya, S.B. and Choudhury, A.,** 2001. Status of sediment with special reference to heavy metal pollution of a brackishwater tidal ecosystem in northern Sundarbans of West Bengal. *Tropical Ecology*, 42(1), pp.127-132.

54. **Schober, P., Boer, C. and Schwarte, L.A.,** 2018. Correlation coefficients: appropriate use and interpretation. *Anesthesia & analgesia*, 126(5), pp.1763-1768.

55. **Sekabira K, Oryem-Origa H, Basamba TA, Mutumba G, Kakudidi E** (2010) Assessment of heavy metal pollution in the urban stream sediments and its tributaries. *Int J Environ Sci Technol* 7(3):435–446. **https://doi.org/10.1007/BF033 26153.**

56. **Sheykhi V, Moore F** (2012) Geochemical characterization of Kor River water quality, fars province, Southwest Iran. Water Qual Expo Health 4(1):25–38. **https://doi.org/10.1007/s12403-012-0063-1**

57. **Sivakumar, B.,** (2011). Global climate change and its impacts on water resources planning and management: assessment and challenges. *Stochastic Environmental Research and Risk Assessment*, 25(4), pp.583-600.

58. **Singh, M., Ansari, A.A., Müller, G. and Singh, I.B.,** 1997. Heavy metals in freshly deposited sediments of the Gomati River (a tributary of the Ganga River): effects of human activities. *Environmental Geology*, 29(3), pp.246-252.

69. **Singh KP, Mohan D, Singh VK, Malik A** (2005) Studies on distribution and fractionation of heavy metals in Gomati river sediments—a tributary of the Ganges, India. *J Hydrol* 312(1–4):14–27. **https://doi.org/10.1016/j.jhydr ol.2005.01.021**

70. **Singh, N.B., Shivani Pandey, S.P. and Ali, S.N.,** 2010. Heavy metal content in Gomati river water, sediment and hydrobiota in Jaunpur.

71. **Singh, R., Tajdarul, A. S. V., & Reddy, H. S. A. G. S.** (2017). Assessment of potentially toxic trace elements contamination in groundwater resources of the coal mining area of the Korba. Environmental Earth Sciences, 76, 566. **https://doi.org/10.1007/s12665-017-6899-8**

72. **Singh, V. K., Singh, K. P.,& Mohan, D.** (2005). Status of Heavy Metals in Water and Bed Sediments of River Gomati –A Tributary of the Ganga River, India. *Environmental Monitoring and Assessment*, 105, (1-3), 43–67. **https://doi.org/10.1007/s10661-005-2816-9.**

73. **Singh, K. P., Malik, A., Sinha, S., Singh, V. K., & Murthy, R. C.** (2005). Estimation of source of heavy metal contamination in sediments of Gomati River (India) using principal component analysis. *Water, Air, and Soil Pollution,* 166(1–4), 321–341. **https://doi.org/10.1007/s11270-005-5268-5**

74. **Singh, K. P., Mohan, D., Singh,V. K., & Malik, A.** (2005). Studies on distribution and fractionation of heavy metals in Gomati river sediments – A tributary of the Ganges, India. *Journal of Hydrology*, 312(1–4), 14–27. **https://doi. org/10.1016/j.jhydrol.2005.01.021**

75. **Srivastava P, Singh IB, Sharma M, Singhvi AK** (2003) Luminescence chronometry and Late Quaternary geomorphic history of the Ganga Plains, India. *Palaeogeogr Palaeoclimatol Palaeoecol* 197:15–41.

76. **Su, K., Wang, Q., Li, L., Cao, R. and Xi, Y.,** 2022. Water quality assessment of Lugu Lake based on Nemerow pollution index

method. *Scientific Reports*, 12(1), p.13613.

77. **Ugochukwu UC, Onuorah AL, Okwu-Delunzu VU et al** (2019) Ecological and human health exposure risks to heavy metals in Oji River sediments: effect of abattoir and power station. *SN Appl Sci* 1:452. **https ://doi.org/10.1007/s4245 2-019-0465-9**

78. **WHO**, (2017). Guidelines for Drinking Water Quality. World Health Organization, Geneva.

79. **Xiao HY, Zhou WB, Wu DS, Zeng FP** (2011) Heavy metal contamination in sediments and floodplain top soils of the Lean river catchment, China. *Soil Sediment Contam* 20:810–823. **https :// doi.org/10.1080/15320383.2011.60920 0**

80. **Yan, C.A., Zhang, W., Zhang, Z., Liu, Y., Deng, C. and Nie, N.** Assessment of water quality and identification of polluted risky regions based on field observations & GIS in the Honghe river watershed, China. *PloS One* 2015; 10: e0119130.

81. **Yuan, H.Z., Shen, J., Liu, E.F., Wang, J.J. and Meng, X.H.,** 2011. Assessment of nutrients and heavy metals enrichment in surface sediments from Taihu Lake, a eutrophic shallow lake in China. *Environmental geochemistry and health*, 33(1), pp.67-81.

82. **Zuhal Abdul and Hadi Hamzah**, Water quality of the Shatt Al-Arab River evaluation using the Nemerow pollution index method. Advances in Science and Technology Research Journal, 2025, 19(5), 14–20, https://doi.org/10.12913/22998624/201132.

83. **Central Water Commission**, Department of Water Resources, Status of Trace and Toxic Metals in Indian Rivers, River Data Compilation-2 Directorate, River Development & Ganga Rejuvenation Ministry of Jal Shakti.